LASERS

PACS numbers: 42.55.Lt; 42.60.Lh
DOI: 10.1070/QE2009v039n08ABEH014027

Electric-discharge VUV laser pumped by a solid-state generator

S.K. Vartapetov, O.V. Gryaznov, M.V. Malashin, S.I. Moshkunov, S.V. Nebogatkin, R.R. Khasaya, V.Yu. Khomich, V.A. Yamshchikov

***Abstract*. A 193-nm electric-discharge ArF laser pumped by an all-solid-state generator based on a semiconductor switch and a system of magnetic compression of high-voltage pulses is studied. The laser emits 18-ns, 15 mJ pulses at a pulse repetition rate of 1 kHz.**

Keywords: *solid-state switch, generator of magnetically compressed high-voltage pulses, long VUV pulse.*

1. Introduction

Electric-discharge ArF and F_2 lasers are high-power VUV radiation sources emitting radiation at 193 nm (6.4 eV) and 157 nm (7.9 eV), respectively [1 – 12], which is absorbed by almost all materials. This radiation can be focused into a spot of diameter $\sim \lambda$, providing the high-intensity local action of a laser beam on materials. The refractive index of optical materials exposed to radiation from ArF and F_2 lasers can be varied, and these lasers are used to form Bragg gratings in optical fibres, which operate as mirrors at the fibre input and output. Optical fibres with Bragg gratings are used in telecommunication. They can be both passive (filters, Raman radiation converters) and active (fibre lasers) elements or can be used as high-sensitive sensors for remote measurements of physical fields, temperatures, pressures, etc. [1, 13 – 16].

ArF and F_2 lasers play a key role in microelectronics. They are used for drilling holes in multilayer integrated printed-circuit boards for computers. As the size of micro-circuits is reduced, the required hole diameter should be a few microns or smaller. Laser radiation at 193 nm is used in the photolithographic technology of last generations for manufacturing integrated circuits with elements as small as 65 – 45 nm [10 – 12]. In addition, due to a high spatial resolution (less than 100 nm) achieved during ablation of solid materials by intense VUV radiation, ArF and F_2 lasers can be efficiently used for the precise processing of materials for manufacturing individual elements of micro-electro-mechanical systems. ArF lasers also have found broad applications in medicine: in ophthalmology for the correction of vision anomalies (myopia, hyperopia, astigmatism) and in dermatology for the medical treatment of skin diseases (psoriasis, eczema) [1]. The possibility of fabricating submicron and nanometre structures on material surfaces by using radiation from a F_2 laser was recently demonstrated in papers [17, 18].

Aside from high output radiation parameters, modern 'industrial' lasers should satisfy a number of additional requirements. They should have high pulse repetition rates up to $\sim$ 1000 Hz, a high beam quality, which is determined by the beam homogeneity, divergence, and spectrum, and also a high reliability, a comparatively small size and weight.

As a rule, either hydrogen thyratrons (the operating life is no less than 10^{10} pulses) or low-voltage solid-state switches with virtually infinite operating life are used in commercial electric-discharge lasers. To improve the operation parameters of industrial lasers, it is necessary to refine solid-state switches.

A number of laser technologies (photolithography, the writing of Bragg gratings in optical fibres, the fabrication of diffraction optical microstructures, etc.) impose advanced requirements to the output beam parameters and the service life of optical elements of a laser setup. In this case, some special problems appear. First, this is a comparatively low monochromaticity and a high divergence of the laser beam. To obtain high spatial and spectral characteristics of radiation, the authors of [3] proposed different schemes of unstable resonators and selection of laser emission spectrum by using dispersion elements. However, such schemes introduce considerable intracavity losses, which reduce the output energy.

Second, high-power VUV radiation causes the compaction of materials. This leads to a change in the refractive index of an optical material (fused silica, fluorite), resulting in the degradation of resonator mirrors and other optical elements through which the laser beam propagates. To solve these problems, it was proposed in [10, 11] to increase the laser pulse duration. In this case, due to the increase in the number of round-trip transits of radiation in the resonator, the spatial coherence of the laser beam is improved and the width of the emission spectrum decreases. In addition, due to the increase in the laser pulse duration, the pulse intensity decreases and the negative influence of material compaction is reduced.

M.V. Malashin, S.I. Moshkunov, S.V. Nebogatkin, R.R. Khasaya, V.Yu. Khomich, V.A. Yamshchikov Institute for Electrophysics and Electric Power, Russian Academy of Sciences, Dvortsovaya naberezhnaya 18, 191186 St. Petersburg, Russia;
e-mail: rutberg@iperas.spb.ru, yamschikov52@mail.ru;
S.K. Vartapetov, O.V. Gryaznov Physics Instrumentation Center, A.M. Prokhorov General Physics Institute, Russian Academy of Sciences, 142190 Troitsk, Moscow region, Russia; e-mail: info@lasersys.ru

Received 10 September 2008; revision received 2 April 2009
Kvantovaya Elektronika **39** (8) 714 – 718 (2009)
Translated by M.N. Sapozhnikov

The aim of this paper is to develop and study a system for pumping small ArF and F_2 lasers (with the active volume of ~ 9 cm^3) with an all-solid-state pump generator generating VUV radiation pulses of duration approximately twice as long as that of conventional lasers and a pulse repetion rate of up to 1 kHz.

2. Magnetic high-voltage pulse generator with a solid-state switch

Characteristics of ArF and F_2 lasers strongly depend on the parameters of high-voltage pulses produced by a pump generator across the discharge gap of a laser. During the voltage growth, a volume self-sustained discharge is ignited which pumps the active medium of the laser. The smaller the duration t_f of the leading edge of the pulse, the more uniform the discharge and the greater the dynamic operating life of the gas mixture[19 – 22].The active medium is excited during the fall of the voltage. As the duration t_p of the voltage fall is decreased, the pump efficiency increases [2, 20, 21]. The value of t_p is usually reduced by minimizing the inductance of the discharge circuit of a peaking capacitor connected in parallel with discharge-gap electrodes. The value of t_f is reduced with the help of peaking circuits [21 – 23]. In the case of repetitively pulsed lasers, the most efficient peaking circuits are magnetic compression systems consisting of a chain of series-connected circuits containing capacitors and nonlinear saturable chokes. The number of successive circuits is chosen to provide the optimally high amplitude and rate of the voltage growth across the discharge gap and to minimize the loss of energy supplied to the discharge gap. The operating life of magnetic compression systems is much longer compared to gas-discharge circuits for high-voltage pulses [21] and these systems can operate at pulse repetition rates higher than 1 kHz [23].

Another very important part of the pump generator is a switch. Recently, high-power semiconductor switches have received wide acceptance. They have virtually unlimited operating life and provide the high stability of voltage pulses. As a rule, pump generators are used with comparatively low-voltage semiconductor switches operating in conjunction with step-up transformers [1]. A high-voltage transformer requires a reliable insulation and for this reason it is usually placed into a tank with the transformer oil. Such devices are rather clumsy, have a large weight and lead to additional energy losses.

Unlike conventional schemes, we developed the circuit of a high-voltage nanosecond pulse generator without a high-voltage transformer. The functional circuit of the generator is shown in Fig. 1. Its specific feature is the use of a high-voltage semiconductor switch proposed in [23]. The generator is assembled based on all-solid-state elements. It contains a high-voltage stabilised voltage supply, a high-voltage solid-state switch (HSS) with a control circuit, a two-circuit system of magnetic pulse compression, and a control unit.

The high-voltage solid-state switch is completely controllable (switching on and switching off) and consists of 32 insulated gate bipolar transistors (IGBTs) switched in parallel and in series. The transistors are controlled with the help of transformers (not shown in Fig. 1). This switching method of IGBTs provides a simple generator circuit with voltage doubling due to an incomplete discharge of a storage capacitor with capacitance C_1.

The high-voltage solid-state switch opens when a control pulse is applied, and capacitor C_2 is charged resonantly through a choke with inductance L_1. The control pulse duration is selected so that the HSS closes at the instant when the maximum voltage is achieved across capacitor C_2. In this case, the current through the HSS is close to zero, which considerably reduces commutation losses. Because $C_1 \gg C_2$, the voltage amplitude across capacitor C_2 tends to the doubled charging voltage $2U_1$. Then, the voltage pulse is sharpened and shortened by the magnetic compression system and is applied to discharge-gap electrodes.

By using a high-voltage 2500-W power supply and forced air cooling, the reliable operation of the generator was demonstrated with an active load of 30 Ω at pulse repetition rates up to 2 kHz, the output pulse amplitudes of 20 – 27 kV, and the pulse front duration ~ 70 ns.

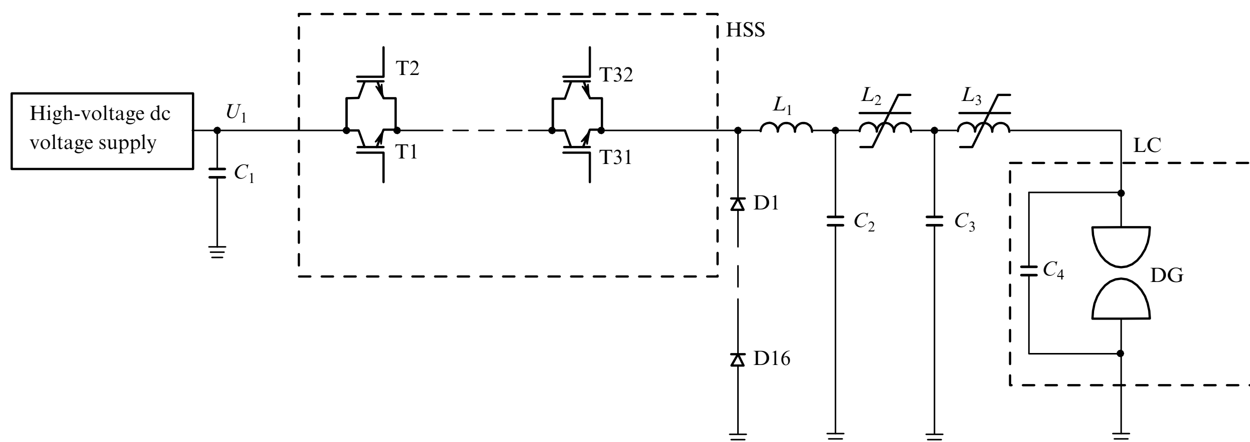

Figure 1. Functional circuit of the pump generator: (C_1) storage capacitor (100 nF, 16 kV); (HSS) high-voltage IGBT switch; (T1 – T32) insulated gate bipolar transistors; (D1 – D16) protective diode array (HFA30PB 120); (L_1) charging choke (23 μH); (C_2) capacitor of the first magnetic compression circuit (3 nF, 32 kV); (L_2) saturable choke of the first magnetic compression circuit (14 μH); (C_3) capacitor of the second magnetic compression circuit (3 nF, 32 kV); (L_3) saturable choke of the second magnetic compression circuit (4 μH); (C_4) peaking capacitor of the laser chamber (2.7 nF); (LC) laser chamber; (DG) discharge gap of the laser.

3. Increasing laser pulse duration

A usual ArF laser emits a short single pulse. In active media of length ~ 30 cm, the laser pulse FWHM is $t_g = 5 - 7$ ns. For the resonator length ~ 30 cm, the number of round-trip transits of radiation in the resonator does not exceed five, which is insufficient for the formation of a highly monochromatic beam. Because of this, the forced elongation of the laser pulse was used in papers [10, 11]. In this case, the output energy should not be reduced and the homogeneity of the discharge in the discharge gap should not be impaired.

The temporal intensity profile of laser pulses is determined by the time dependence of the electric power supplied to the active medium. In the case of a short laser pulse, the value of t_g is determined by the time of discharge of the peaking capacitor (connected to the discharge-gap electrodes) through the discharge gap. To generate laser pulses of a longer duration, the authors of [11] proposed the electric circuit shown in Fig. 2. This scheme uses instead of the peaking capacitor an artificial formation line consisting of capacitors C_{p-1} and C_p and nonlinear inductance L. The passage of inductance L to the saturated state causes the 'flow' of the accumulated energy from C_{p-1} to C_p and an increase in the voltage across the discharge gap. After the discharge gap breakdown, both capacitors are discharged alternately through the discharge gap. If the energies in C_{p-1} and C_p are approximately equal during the discharge, a laser pulse with two peaks is generated. The ratio of their amplitudes depends on the capacity C_p, the fluorine concentration, and mixture pressure.

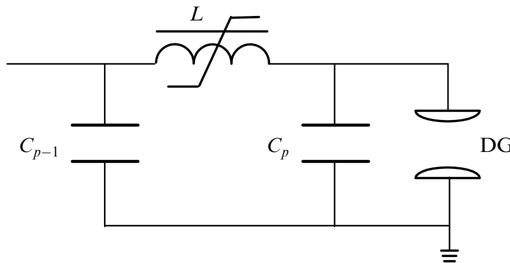

Figure 2. Electric excitation circuit for generating laser pulses of a longer duration.

A comparison of Figs 1 and 2 shows that the circuit consisting of the output circuit (C_3, L_3) of the generator and capacitor C_4 (Fig. 1) is in fact the formation line, which is similar to that shown in Fig. 2. Therefore, the high-voltage nanosecond pulse generator, schematically shown in Fig. 1, can be obviously used for pumping required to generate a longer laser pulse.

4. Experimental setup

A system for pumping an electric-discharge VUV laser contained a solid-state magnetic pump generator and a laser chamber (Fig. 1). The laser chamber was earlier used in a F_2 laser and is described in [6]. We performed experiments with an ArF laser. The active volume of the discharge gap was $V = dwl$, where $d = 1.2$ cm is the interelectrode gap, $w = 0.3$ cm is the discharge width, and $l = 25$ cm is the discharge length.

The optical resonator of length 34 cm was mounted on the laser chamber housing. The resonator was formed by a highly reflecting plane mirror and a plane-parallel CaF_2 plate output window.

The $F_2 - Ar - He - Ne$ gas mixture was pumped through the discharge gap with the help of a diametral fan. The mixture pressure in the laser chamber did not exceed 5000 bar. The working mixture was cooled by running water. The diametral fan and water cooling radiator were mounted inside the laser chamber.

The output laser energy was measured with an Ophir pyroelectric detector. The voltage pulses of the pump generator across the discharge gap and laser pulses were detected simultaneously by using a Tektronix P6015A high-voltage probe, a FEK-22 coaxial photocell, and a LeCroy WaveSurfer 432 oscilloscope.

The mixture composition and pressure were optimised to obtain the maximum output power at a pulse repetition rate of 10 Hz. For the charging voltage $U_1 = 12$ kV, the optimal relation between the components of the $F_2 - Ar - Ne$ mixture was found for its total pressure of 4630 mbar.

5. Output laser parameters

Figures 3 and 4 present the experimental dependences of the laser radiation energy W, the maximum voltage U_m across the discharge gap, and the voltage pulse FWHM $t_{1/2}$ on the charging voltage U_1 of the pump generator for the optimal gas mixture.

Figure 5 shows the oscillograms of voltage pulses across the discharge gap and 193-nm laser pulses for different values of U_1. They demonstrate the evolution of the laser pulse with changing the charging voltage. For $U_1 = 10$ kV,

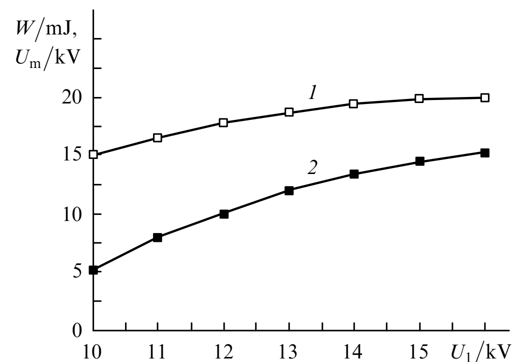

Figure 3. Experimental dependences of the maximum voltage U_m across the discharge gap (*1*) and the laser output energy W (*2*) on the charging voltage U_1.

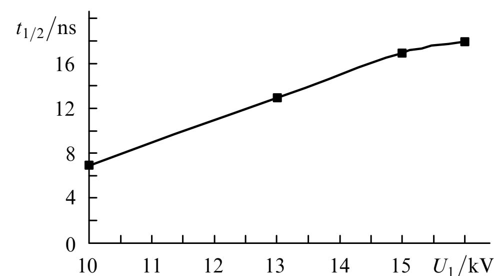

Figure 4. Experimental dependence of the laser pulse FWHM $t_{1/2}$ on the charging voltage U_1.

the voltage pulse has a flat top. This means that the discharge-gap breakdown occurs during the time period when the total pump energy is concentrated in the capacitor C_4. As a result, the laser pulse represents a single peak whose shape is determined only by the discharge of the capacitor C_4 through the discharge gap. In the range $U_1 = 10 - 12$ kV, the discharge voltage amplitude U_m increases linearly. This leads to the increase in the laser pulse amplitude. Due to the decrease in the breakdown delay time of the discharge gap with respect to the instant of the voltage-pulse front growth for $U_1 \geqslant 12$ kV, the breakdown occurs at the voltage pulse front. Under these conditions, the pump energy is determined by the discharges of capacitors C_3 and C_4. As a result, for $U_1 = 13$ kV, a laser pulse with two peaks is observed (Fig. 5b), which is caused by the discharge of both capacitors. One can see from Fig. 3 that, as U_1 is further increased, the value of U_m increases insignificantly. Because of this, the amplitude of the first peak also changes insignificantly, while the amplitude of the second peak grows and even can exceed the amplitude of the first peak. In this case, the value of $t_{1/2}$ becomes approximately equal to the doubled duration of a single peak, achieving 18 ns for $U_1 = 16$ kV.

Our investigations showed that the laser operated stably at a pulse repetition rate $f < 1$ kHz. The maximum lasing efficiency with respect to the energy stored in the capacitor C_2 (Fig. 1) was 1.2% for the charging voltage 13 kV. The dependence of the output energy on the pulse repetition rate for the charging voltage 15 kV is shown in Fig. 6. The output energy for $f = 1000$ Hz decreased by 15 % with respect to the output energy for $f = 20$ Hz. In this case, the average output power exceeded 10 W.

We developed earlier the efficient system for exciting an electric-discharge F_2 laser, which was investigated in detail in [6]. As a whole, this system is similar to that discussed in the present paper. The same laser chamber was used in it, but with the optical resonator for 157 nm. The switch in the pump generator was a TPI1-1k/20 cold thyratron. Despite some difference in pulse magnetic compression schemes, the parameters of voltage pulses across the discharge gap obtained in [6] and this paper were close. We have failed to record the 157-nm pulse shape because of the presence of the red emission (624 – 755 nm) of atomic fluorine F^* in the emission spectrum of the F_2 laser [2, 5]. Nevertheless, it was shown in [11] that the principle of generating longer laser pulses based on the discharge of a nonlinear formation line through the discharge gap can be used both for ArF and F_2 lasers. Therefore, the excitation scheme considered in this paper can be also used for generating 157-nm laser pulses of a longer duration.

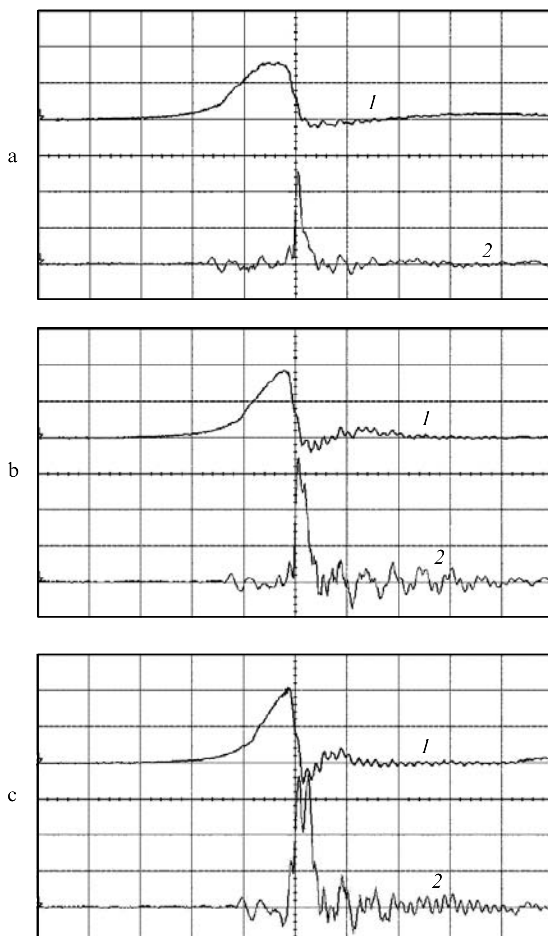

Figure 5. Oscillograms of discharge voltage (*1*) and laser (*2*) pulses for the charging voltage $U_1 = 10$ (a), 13 (b), and 16 kV (c). The scale for oscillograms (*1*) is 10 kV div^{-1}; oscillograms (*2*) are presented in relative units; the scan is 50 ns div.$^{-1}$

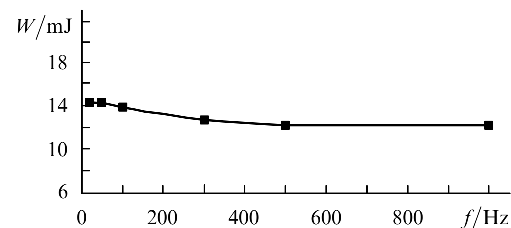

Figure 6. Dependence of the output laser energy W on the puse repetition rate f for $U_1 = 16$ kV.

6. Conclusions

Thus, we have developed the efficient system for excitation electric-discharge VUV lasers, which is based on the use of all-solid-state magnetic pump generator. The system allows the generation of long (up to 18 ns) ArF laser pulses of energy up to 15 mJ. The average radiation power at 193 nm achieves more than 10 W at a pulse repetition rate of 1 kHz.

Acknowledgements. This work was supported by the Russian Foundation for Basic Research (Grant Nos 08-08-00784-a and 08-08-00965-a).

References

1. Basting D. et al (Eds). *Excimer Laser Technology* (Göttingen: Lambda Physik AG, 2001).
2. Atezhev V.V., Vartapetov S.K., Zhukov A.N., Kurzanov M.A., Obidin A.Z., Yamshchikov V.A. *Kvantovaya Elektron.*, **33**, 677 (2003) [*Quantum Electron.*, **33**, 677 (2003)].
3. Atezhev V.V., Vartapetov S.K., Zhukov A.N., Kurzanov M.A., Obidin A.Z., Yamshchikov V.A. *Kvantovaya Elektron.*, **33**, 689 (2003) [*Quantum Electron.*, **33**, 689 (2003)].

4. Atejev V.V., Vartapetov S.K., Zhukov A.N., Kurzanov M.A., Obidin A.Z., Yamschikov V.A. *Tech. Program XI Conf. on Laser Opt.* (St. Petersburg, 2003) p. 18.
5. Atejev V.V., Vartapetov S.K., Zhukov A.N., Kurzanov M.A., Obidin A.Z., Yamschikov V.A. *Proc. SPIE Int. Soc. Opt. Eng.*, **5479**, 123 (2004).
6. Vartapetov S.K., Zhigalkin A.A., Lapshin K.E., Obidin A.Z., Khomich V.Yu., Yamshchikov V.A. *Kvantovaya Elektron.*, **36**, 393 (2006) [*Quantum Electron.*, **36**, 393 (2006)].
7. Khomich V.Yu., Yamshchikov V.A. *Elektron. Zh. 'Issledovanno v Rossii'*, **152**, 1414 (2006).
8. Peters P., Feenstra L., Bastiaens H. *Proc. SPIE Int. Soc. Opt. Eng.*, **4184**, 338 (2001).
9. Borisov V., Khristoforov O., Kirykhin Yu., Vinokhodov A., Demin A., Vodchits V., Eltzov A. *Proc. SPIE Int. Soc. Opt. Eng.*, **4184**, 348 (2001).
10. Kakizaki K., Saito T., Mitsuhashi K., Arai M., Tada T., Kasahara S., Igarashi T., Hotta K. *Proc. SPIE Int. Soc. Opt. Eng.*, **4000**, 1397 (2000).
11. Hofmann T., Johanson B., Das P. *Proc. SPIE Int. Soc. Opt. Eng.*, **4000**, 511 (2000).
12. Klerk J., Wagner C., Droste R., Levasier L., Jorritsma L., Setten E., Kattouw H., Jacobs J., Tilmann Heil T. *Proc. SPIE Int. Soc. Opt. Eng.*, **6520**, 65201Y (2007).
13. Othonos A., Kalli K. *Fiber Bragg Gratings: Fundamentals and Applications in Telecommunications and Sensing* (Boston, London: Artech House, 1999).
14. Larionov Y., Rybaltovsky A., Semjonov S., Bubnov M., Dianov E., Vartapetov S., Kurzanov M., Obidin A., Yamschikov V. *Tech. Dig. Conf. on Optical Fiber Communication (OFC-2003)* (Atlanta, GA, USA, 2003) Vol. 1, p. 38.
15. Larionov Yu.V., Rybaltovsky A.A., Semjonov S.L., Bubnov M.M., Dianov E.M., Vartapetov S.K., Kurzanov M.A., Obidin A.Z., Yamschikov V.A. *Tech. Dig. Conf. on Bragg Gratings, Photosensitivity and Poling in Glass Waveguides (BGPP'2003)* (Monterey, CA, USA, 2003) MD28, p. 136.
16. Larionov Yu.V., Rybaltovsky A.A., Semjonov S.L., Bubnov M.M., Dianov E.M., Vartapetov S.K., Kurzanov M.A., Obidin A.Z., Yamschikov V.A., Guryanov A.N., Yashkov M.V., Umnikov A.A. *Tech. Dig. Conf. on Bragg Gratings, Photosensitivity and Poling in Glass Waveguides (BGPP'2003)* (Monterey, CA, USA, 2003) MC4, p. 46.
17. Lapshin K.E., Obidin A.Z., Tokarev V.N., Khomich V.Yu., Shmakov V.A., Yamshchikov V.A. *Ross. Nanotekh.*, **2**, 59 (2007).
18. Lapshin K.E., Obidin A.Z., Tokarev V.N., Khomich V.Yu., Shmakov V.A., Yamshchikov V.A. *Fiz. Khim. Obrab. Mater.* (1), 35 (2008).
19. Osipov V.V. *Usp. Fiz. Nauk*, **170**, 225 (2000).
20. Mesyats G.A., Osipov V.V., Tarasenko V.F. *Impul'snye gazovye lazery* (Pulsed Gas Lasers) (Moscow: Nauka, 1991).
21. Mesyats G.A. *Generirovanie moshchnykh nanosekundnykh impul'sov* (Generation of High-power Nanosecond Pulses) (Moscow: Sov. Radio, 1974).
22. Apollonov V.V., Yamshchikov V.A. *Kvantovaya Elektron.*, **24**, 483 (1997) [*Quantum Electron.*, **27**, 469 (1997)].
23. Ivanov E.V., Moshkunov S.I., Khomich V.Yu. Preprint IPEF, RAS (Moscow, 2004).